ADVANCED MATERIALS
www.advmat.de

Single-Fiber-Based Hybridization of Energy Converters and Storage Units Using Graphene as Electrodes

Joonho Bae, Young Jun Park, Minbaek Lee, Seung Nam Cha, Young Jin Choi, Churl Seung Lee, Jong Min Kim, and Zhong Lin Wang**

Recently, there has been great interest in wearable and stretchable energy generation and storage devices utilizing nanotechnology for applications such as self-powering nanosystem that harvests its operating energy from the environment.[1] Solar, mechanical and thermal energy can be scavenged from the environment using devices that were fabricated using flexible or stretchable substrates. For example, textile-fibre-based nanogenerators have been demonstrated utilizing ZnO nanowires (NWs) grown on Kevlar fibres to scavenge low-frequency mechanical energy.[2] Twisted fibre-like electrodes have been used for harvesting solar energy using the dye-sensitized solar cells (DSSCs) approach.[3] Once the energy is harvested from the environment, an energy storage device is required in order to maintain the operation of the system, but it is usually a separated unit from the energy converters. Flexible batteries.[4] and electrochemical double-layer capacitors or supercapacitors are typical energy storage for flexible electronics.[5] Herein, we report the first prototype of fabricating and integrating the hybrid energy converters and storage devices along a single micro size fibre using ZnO nanowires (NWs) and graphene as the basic materials. Such a power fiber system can simultaneously scavenge both mechanical and solar energy, and store it in a nanowire-based supercapacitor. Our device demonstrates the feasibility of integrating multi-functional devices on a single plastic fiber for potential applications of driving other nanodevices by harvesting energy from environment, and it is a great step toward building self-powering system.

The design of the power fiber is presented in **Figure 1**, which includes a nanogenerator, a DSSC and supercapacitor, all of which are built along one micro-size fiber. The radially grown ZnO nanowires (NWs) are the acting units for the nanogenerator (NG) that harvests mechanical energy[6–9] and the core of the DSSC as well as the supercapacitor (SC) with large surface area. Graphene is used as the cylindrical electrodes for NG, DSSC and SC. Importantly, ZnO NWs can be grown easily on fibres at a low temperature (less than 90 °C) via chemical approach. Graphene is a great electrode material[10–13] with high conductivity and transparency. A SEM image and Raman spectra of the prepared graphene are shown in Figure 1a and Figure 1b. The distinct G- and 2D-peaks are observed in the Raman spectrum at ~1600 cm^{-1} and 2700 cm^{-1}, respectively, with the negligible D-peak, indicating that the graphene used here is of high quality without critical defects.

The entire fabrication was based on a single polymethyl methacrylate (PMMA) fibre of diameter ~220 μm. The surface of the fibre was first covered by a layer of Au to serve as a common electrode. Then, quasi-aligned ZnO NW arrays were grown by a chemical approach. These structures are shared by the three devices to be built one by one. Figure 1c shows a low magnification SEM image of a plastic wire covered with ZnO NWs. The close-up view on the NWs is shown in the inset in Figure 1b. The as-grown ZnO NWs on the plastic wire show typical hexagonal flat ended, indicating their growth direction being c-axes. The diameters of a NW range from 500 to 700 nm, and the lengths are about 6 μm. Copper meshes covered with graphene were employed as distinct electrodes for each energy harvesting and storage devices, which were carefully wrapped around the fiber. The resistance of the device was monitored during the entangling process to ensure the two electrodes were not in contact with each other.

After the plastic wire covered with ZnO NWs and graphenes on Cu mesh were prepared, our multi-energy devices have been fabricated by wrapping graphenes around the plastic wire (Figure 1). For DSSC part and supercapacitor part, liquid electrolyte and gel electrolyte were filled in between Cu mesh and the plastic wire for DSSC and supercapacitor part, respectively.

The first device built on the fiber is a nanogenerator that converts mechanical energy into electricity with the use of piezoelectric property of ZnO. The size of the nanogenerator part is about 5 mm long. We measured the current output generated from the nanogenerator part using graphene as the top electrode by applying a pushing force. Manually driven pushing action (~5 Hz) delivered a shear stress between ZnO NWs and

Dr. J. Bae, M. Lee, Prof. Z. L. Wang
School of Materials Science and Engineering
Georgia Institute of Technology
Atlanta, GA, 30332, USA
E-mail: zlwang@gatech.edu
Y. J. Park, S. N. Cha, Dr. J. M. Kim
Frontier Research Lab
Samsung Advanced Institute of Technology
Samsung Electronics
Gyeonggi-Do 446–712, Korea
E-mail: jongkim@samsung.com
Prof. Y. J. Choi
Department of Physics
MyongJi University
Yongin, 449–728, Korea
Department of Nano Science and Engineering
MyongJi University
Yongin, 449–728, Korea
Dr. C. S. Lee
Energy Nanomaterials Research Center
Korea Electronics Technology Institute
68 Yatap-dong, Bundang-gu, Seongnam-si, Gyeonggi-do, 463–816, Korea

DOI: 10.1002/adma.201101345

ADVANCED MATERIALS
www.advmat.de

www.MaterialsViews.com

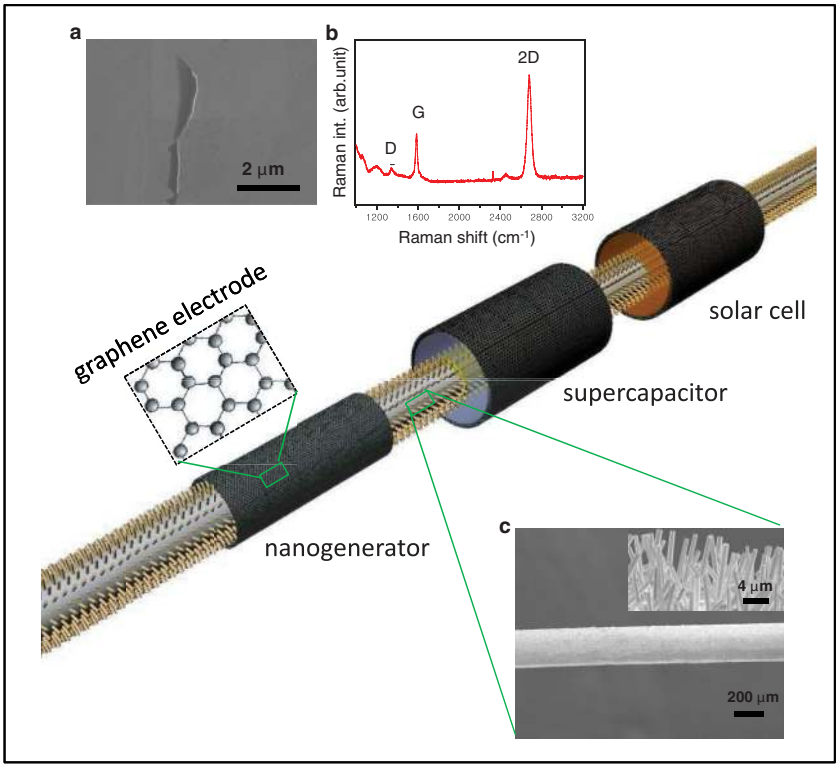

Figure 1. Schematic of fiber-based multi-energy device comprising of a nanogenerator (mechanical energy harvesting), solar cell (solar energy harvesting) and supercapacitor (electrochemical charge storage). ZnO NWs are grown on a flexible thin plastic wire coated with thin Au film. High-quality conductive and transparent graphenes on Cu mesh were used as electrodes for each energy devices. For solar cell, and supercapacitor, the corresponding electrolytes were filled in between ZnO NWs and graphene electrodes. (a) SEM image of a graphene film. (b) Raman spectra of the graphene film. (c) Low resolution SEM image of Au-coated plastic wire covered with ZnO NW arrays. The inset is a SEM image of the plastic wire showing ZnO NW arrays grown along the radial direction.

graphene electrode with a strain of ~0.1% (see Figure S3 in the Supporting Information), which resulted in periodic friction motions between NWs and electrode. As shown in **Figure 2**c, the short-circuit current was successfully detected with sharp current peaks in responding to the mechanical agitation. The maximum output current from the nanogenerator was approximately 2 nA. Maximum open-circuit voltage was also measured to be about 7 mV (Figure 2d). The high carrier mobility.[14] (μ_c = 1760 cm^2 W^{-1} S^{-1}) of the graphene electrode may have contributed to the high on/off ratio of the nanogenerator part of our multi-energy devices.[14]

For a working nanogenerators, there must be a Schottky barrier at the contact between ZnO NWs and the top electrode.[2,9] The ZnO NWs grown on plastic wire in our experiments were oriented along the c-axis. The work function of the graphene electrode is measured to be 4.4–4.7 eV.[15] Since the electron affinity of ZnO is 4.1–4.35 eV.[16] a Schottky contact is formed at the interface between graphene and a ZnO NW (Figure 2b). Details about the characteristics of the output signals are given in the Supporting Information.

DSSC is the second device fabricated around the fiber with the use of high quality graphene with good transparency. Thermal and chemical stabilities of graphenes also make them attractive as an alternative to the conventional metal oxide window materials for DSSCs.[17] Based on the structure shown in Figure 1, the dye molecules are placed in between ZnO NWs and the bottom electrode on the fiber. A liquid electrolyte was injected between the fiber and the top graphene electrode. Since the dye is in liquid form, eventually it will be mixed up with the liquid electrolytes in between ZnO NWs and the bottom electrode. The electrolyte has to be effective to separate the two electrodes. The effective length and area of the plastic wire wrapped with graphenes were 5 mm, and 0.035 cm^2, respectively. **Figure 3**c shows plot of current density as a function of voltage (J–V curve). The short-circuit current density J_{sc}, open-circuit voltage V_{oc} were determined to be 0.35 mA/cm^2, and 0.17 V, respectively. The fill factor FF was 0.39. Hence, the energy conversion efficiency is 0.02%. The low energy conversion efficiency is mainly attributed to the use of Cu mesh that is not fully transparent, resulting in a significant loss in the transfer of light energy to the dyes. To improve the DSSCs performance, graphenes on the transparent substrates or direct packaging of graphenes in the DSSCs without any substrates would be necessary.

The supercapacitor part is comprised of two electrodes, which employed a ZnO NWs on the plastic wire and graphenes on Cu mesh, with polymer gel electrolyte (PVA/H_3PO_4) filled between. While most electrolytes in electrochemical devices are in the liquid form, solid gel electrolytes have been

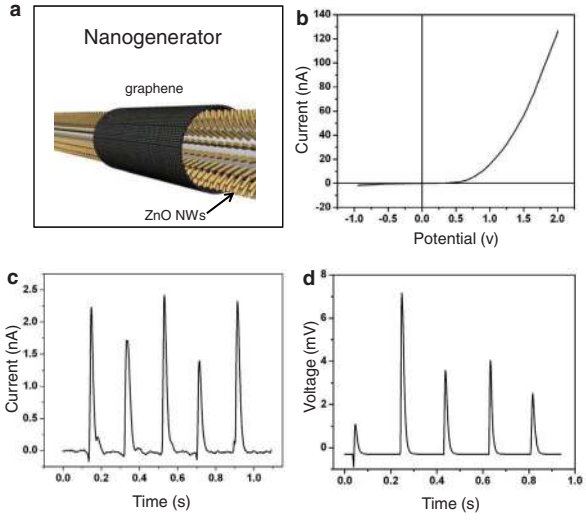

Figure 2. (a) Schematic of nanogenerator part in the multi-energy device. (b) SEM image of ZnO NWs grown on graphene. (c) Current-voltage plot showing the Schottky contact between ZnO NWs and graphene top electrode. (d) The short-circuit output current, and (d) open-circuit output voltage of the nanogenerator.

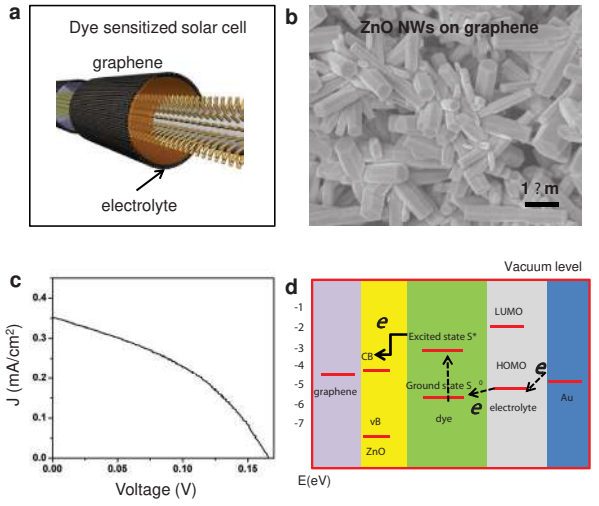

Figure 3. (a) Schematic of DSSC part in the multi-energy device. (b) SEM image of ZnO NWs grown on graphene. (c) *J–V* curves of the DSSC under one full-sun illumination. The illumination is normal to the plastic wire. (d) Energy level diagram of graphene/ZnO NWs/dye/electrolyte/Au DSSC.

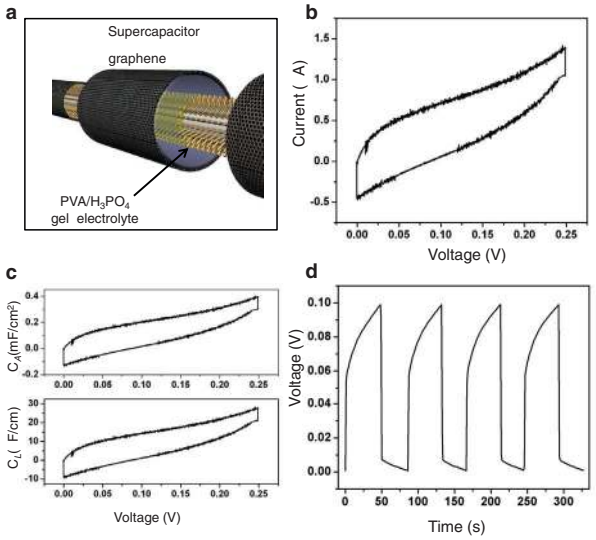

Figure 4. (a) Schematic of supercapacitor part using graphene and gel electrolyte. (b) Typical cyclic voltammetry of supercapacitor part using PVA/H_3PO_4 as electrolyte at 100 mV/s. (c) Upper figure: area specific capacitance (C_A) of the supercapacitor at 100 mV/s. Bottom figure: length specific capacitance (C_L) of the supercapacitor at 100 mV/s. (d) Galvanostatic charge-discharge curve measured with a 1 μA.

recently explored as alternative electrolytes. Solid gel or polymer electrolytes were reported to combine the separator and the electrolyte into a single layer while liquid electrolytes require a separator to avoid electrical contact between the electrodes. In order to make our fiber-based energy devices with supercapacitors fully wearable, the electrolytes need to be fully encapsulated in the devices without any leakage. In this regards, using of solid gel electrolytes are more preferable than any conventional liquid electrolytes such as KNO_3 or H_2SO_4 for future applications of our fiber multi-energy device.

Cyclic voltammetry from the supercapacitor part shows good electrochemical stability and capacitance of fibre-based electrochemical capacitors (**Figure 4**b). The scan range is between 0 and 250 mV with scan rates of 100 mV/s. From Figure 4b, the capacitance as a function of potential at a voltage scan rate of 100 mV/s can be easily obtained, and is shown in Figure 4c. The area specific capacitance can be calculated from cyclic voltammograms (Figure 4b) using the equation of $C = Q/V/A = I/S/A$, where C is the capacitance (F), Q is the charge (C) accumulated in the capacitors, V is the potential (V) in CV curve, I is the current (A) in CV curve, S is the voltage scan rate (V/s), and A is the effective area of supercapacitor (0.035 cm^2). The calculated area specific capacitance is shown in the upper part in Figure 4c. This area specific capacitance curve reveals that the specific capacitance of fiber supercapacitors reached up to ~0.4 mF/cm^2 at a voltage scan rate of 100 mV/s. Micro-supercapacitors were reported to demonstrate an area specific capacitance of 0.4–2 mF/cm^2, [17–21] indicating that the capacitance value of 0.4 mF/cm^2 of our device is slightly lower than those in the literature. Further optimization would be necessary to increase the specific capacitances of fiber supercapacitors. For instance, matching the pore sizes and solvated ion sizes of electrolytes, and controlling the density of ZnO NWs.[22] is very critical to obtain the high performance of electrochemical capacitors.

The conventional capacitors have two-dimensional plate-like substrates. Since our fiber supercapacitors possess unique one-dimensional shape substrates, capacitance per unit length (mF/cm) would be a useful parameter to characterize the capacitance behavior of the devices. In this regard, we calculated the capacitance per unit length by dividing the capacitance in Figure 4c by the effective length of the device (5 mm). The bottom figure in Figure 4c reveals that the capacitance per unit length reached up to about 0.025 mF/cm. The galvanostatic charge-discharge measurement was also conducted to characterize the electrochemical capacitor performance of the fiber supercapacitors, and the curve is shown in Figure 4d. To obtain this curve, charge-discharge current was kept constant at 1 μA. A typical triangular shape of these charge-discharge curves suggests that the capacitance of our fiber supercapacitors is originated from the effective ion adsorption at the interface of electrolyte/ZnO NWs.

In summary, we demonstrated the first integration of multiple energy harvesters and storage device along a single fiber suing ZnO nanowires (NWs) and graphenes as the basic materials, which allows a simultaneous harvesting of solar and mechanical energies. The unique architecture of fiber-based electrodes, use of ZnO NWs, and graphenes as active material and electrodes, could be useful for the future development of flexible and wearable electronics. In addition, the methodology demonstrated here would be applicable to develop other fiber-based electronic circuits or power-shirt when flexibility and stretchability are required.

Experimental Section

Graphene was synthesized using thermal chemical vapor deposition (CVD) on a Cu mesh substrate (purchased from TWP Inc.). The Cu mesh has 150 meshes having each mesh with diameter of 0.0026 m. After the substrate was placed in the CVD chamber, the chamber was

evacuated down to a pressure of 10 mTorr, and filled with H_2 gas at a flow rate of 4 sccm. Then the temperature was increased to 985 °C from room temperature. The synthesis of the graphene occurred at a flow rate of CH_4 at 40 sccm. The growth time was 10 min. After the growth was completed, the chamber was cooled to room temperature. The CVD growth of hydrocarbons has shown some promise in growing large-area graphene on metal substrates such as Ni and Cu.[23]

The ZnO NWs on plastic wire were prepared as follows. A plastic wire was cleaned with DI water, and deposited with Au film of 300 nm thick by using an RF magnetron sputter. Au film on the wire was used as a seed layer to grow ZnO NWs and common metal electrodes for each device, simultaneously. The ZnO NWs were grown by using the typical chemical approach. The growth solution was prepared at 2.5 mM by dissolving zinc nitrate hexahydrate (98%, Aldrich) and hexamethylenetetramine (HMTA) (99%, Aldrich) in deionised water. Then, the Au coated plastic wires were dipped in a glass bottle filled with the growth solution. The growth temperature was 80 °C, and typical growth time was 18 h. The surface morphology of ZnO NWs was characterized by using a field emission scanning electron microscope (SEM, LEO 1550).

The DSSC part of multi-energy devices employed graphene film on Cu mesh as anode and Au on ZnO NWs as cathode. To grow ZnO NWs on graphene, the solution of ZnO seed particles were drop-coated on graphene. The seed particle solution was 5 mM zinc acetate $[Zn(C_2H_3O_2)_2]$ in ethanol. The ZnO seed particle deposited graphene were thermally annealed at 300 °C for 5 min. The growth of ZnO NWs on the graphene was performed using the same chemical method as ZnO NWs growths on the plastic wire as described earlier. The DSSC part was fabricated as follows. Firstly, the ZnO NWs on the plastic wire were sensitized in a 0.5 mM N719 dye solution in dry ethanol for 7 h. A ZnO NWs-grown graphene sheet was employed as the counter electrode. The internal space of the device was filled with a liquid electrolyte (0.5 mLiI, 50 mm I2, 0.5m 4-tertbutylpyridine in 3-methoxypropionitrile) by the capillary effect. The entire cell was fully packaged and covered to prevent light leakage. The solar cell was irradiated using a solar simulator (300 W Model 91160, Newport) with an AM 1.5 spectrum distribution calibrated against a NREL reference cell to accurately simulate a full-sun intensity (100 mW/cm^2). For supercapacitor part, poly(vinyl alcohol) (PVA) powder (10 g) was mixed with water (100 mL) and phosphoric acid (10 g) to prepare the gel electrolyte. The electrochemical properties of our capacitors in the gel electrolyte were characterized using a potentiostat/galvanostat (Princeton Applied Research VersaStat 3F).

Acknowledgements

J.B. and Y.J.P. contributed equally to this work. Research was supported by Samsung. C.Y.J. thanks support by the Ministry of Knowledge Economy (MKE) through the National Platform Technology Program (grant 10033707).

Received: April 10, 2011
Published online:

[1] Z. L. Wang, Scientific American, January issue **2008**, 82–87.
[2] Y. Qin, X. Wang, Z. L. Wang, *Nature* **2008**, *451*, 809.
[3] X. Fan, Z. Chu, F. Wang, C. Zhang, L. Chen, Y. Tang, D. Zou, *Adv. Mater.* **2008**, *20*, 592.
[4] *Flexible primary thin film battery*, www.powerpaper.com (accessed June 2011).
[5] M. Kaempgen, C. K. Chan, J. Ma, Y. Cui, Y. G. Gruner, *Nano Lett.* **2009**, *9*, 1872.
[6] Q. Wan, Q. H. Li, Y. J. Chen, T. H. Wang, X. L. He, J. P. Li, C. L. Lin, *Appl. Phys. Lett.* **2004**, *84*, 3654.
[7] B. Weintraub, Y. G. Wei, Z. L. Wang, *Angew Chem.* **2009**, *48*, 8981.
[8] J. Goldberger, D. J. Sirbuly, M. Law, P. Yang, *J. Phys. Chem. B* **2005**, *109*, 9.
[9] Z. L. Wang, J. Song, *Science* **2006**, *312*, 242.
[10] A. R. Schlatmann, D. W. Floet, A. Hilberer, F. Garten, P. J. M. Smulders, T. M. Klapwijk, G. Hadziioannou, *Appl. Phys. Lett.* **1996**, *69*, 1764.
[11] J. C. Scott, J. H. Kaufman, P. J. Brock, R. DiPietro, J. Salem, J. A. Goitia, *J. Appl. Phys.* **1996**, *79*, 2745.
[12] A. Andersson, N. Johansson, P. Böms, N. Yu, D. Lupo, W. R. Salaneck, *Adv. Mater.* **1998**, *10*, 859.
[13] L. Wang, Y. Yang, T. J. Marks, Z. F. Liu, S. T. Ho, *Appl. Phys. Lett.* **2005**, *87*, 161107.
[14] a) K. S. Kim, Y. Zhao, H. Jang, S. Y. Lee, J. M. Kim, K. S. Kim, J.-H. Ahn, P. Kim, J.-Y. Choi, B. H. Hong, *Nature* **2009**, *457*, 706; b) D. Choi, M. Choi, W. M. Choi, H. Shin, H. Park, J. Seo, J. Park, S. Yoon, S. J. Chae, Y. H. Lee, S. Kim, J. Choi, S. Y. Lee, J. M. Kim, *Adv. Mater.* **2010**, *22*, 2187.
[15] R. Czerw, B. Foley, D. Tekleab, A. Rubio, P. M. Ajayan, D. L. Carroll, *Phys. Rev. B* **2002**, *66*, 033408.
[16] B. J. Coppa, R. F. Davis, R. J. Nemanich, *Appl. Phys. Lett.* **2003**, *82*, 400.
[17] X. Wang, L. Zhi, K. Mullen, *Nano Lett.* **2008**, *8*, 323.
[18] C. J. Lee, T. J. Lee, S. C. Lyu, Y. Zhang, H. Ruh, H. J. Lee, *Appl. Phys. Lett.* **2002**, *81*, 3648.
[19] H. J. In, S. Kumar, Y. Shao-Horn, G. Barbastathis, *Appl. Phys. Lett.* **2006**, *88*, 0831041.
[20] D. Pech, M. Brunet, P. Taberna, P. Simon, N. Fabre, F. Mesnilgrente, V. Conédéra, H. Durou, *J. Power Sources* **2010**, *195*, 1266.
[21] M. Kaempgen, C. K. Chan, J. Ma, Y. Cui, G. Gruner, *Nano Lett.* **2009**, *9*, 1872.
[22] S. Xu, C. S. Lao, B. Weintraub, Z. L. Wang, *J. Mater. Res.* **2008**, *23*, 2072.
[23] X. Li, W. Cai, J. An, S. Kim, J. Nah, D. Yang, R. Piner, A. Velamakanni, I. Jung, E. Tutuc, S. J. Banerjee, L. Colombo, R. S. Ruoff, *Science* **2009**, *324*, 1312.